J Ther Eng, Vol. 10, No. 3, pp. 541−551, May, 2024

Journal of Thermal Engineering
Web page info: https://jten.yildiz.edu.tr
DOI: 10.14744/thermal.0000812

Research Article

Numerical simulation of non-linear film variation and heat transfer characteristics in falling film evaporation around in-line horizontal tubes

Awdhesh Kumar PODDAR[1], Nirmal Kant SINGH[1,*]

[1]*Department of Mechanical Engineering, NIT Kurukshetra, 136119, India*

ARTICLE INFO

Article history
Received: 06 May 2022
Revised: 08 August 2022
Accepted: 09 December 2022

Keywords:
Falling Film; Film Thickness; Heat Transfer; Horizontal Tube

ABSTRACT

In falling film evaporation on a horizontal tube, heat transfer phenomena are highly unpredictable due to uncertainties in the determination of film thickness around the tube, local dry-out condition, geometrical configuration, tube spacing etc. Numerical simulations of falling film evaporation around a single horizontal tube are performed using volume of fluid (VOF) method. Film thickness around the circumference of the horizontal tube is investigated and validated with Nusselt correlations and experiments carried out by researchers. The results are in good agreement with experimental investigations performed by various researchers. Influence of inter-tube spacing, film Reynolds number and variation of diameter on the formation of film thickness are studied and it is found that the film thickness is minimum around 100°-120° circumferential position, whereas Nusselt correlation predicted the minimum value at 90° circumferential position. Wall shear stress and heat transfer are also studied around the horizontal cylinder. It is seen that near the impingement zone, fluctuation of wall shear stress and heat transfer are very high, showing abnormal behaviour in this zone.

Cite this article as: Poddar AK, Singh NK. Numerical simulation of non-linear film variation and heat transfer characteristics in falling film evaporation around in-line horizontal tubes. J Ther Eng 2024;10(3):541−551.

INTRODUCTION

Fluid motion, boiling, and condensation are classified as forms of the convection mode of heat transfer. In an evaporative heat transfer process, the phase change process occurs without influencing the fluid temperature. In this phenomenon, a large heat transfer rate may be achieved with small temperature differences. Falling film evaporation is of great importance in the area of the food industry, seawater desalination, and pharmaceutical industries [1-3]. A schematic diagram of an evaporative heat exchanger is shown in Figure 1, where three horizontal cylinders are placed in line with desired spacing and a water distributor is placed on top of the cylinders.

This is a heat transfer process in which the fluid sprayed over a heated tube is allowed to evaporate. The heat exchange process is carried out at a very low-temperature gradient in this type of heat exchanger [4]. The enhanced surface of the tube and geometrical arrangement is also an interesting area of research. A number of theoretical and experimental studies have been carried out to optimize

***Corresponding author.**
*E-mail address: akpm25@gmail.com, nksinghfme@nitkkr.ac.in

This paper was recommended for publication in revised form by Regional Editor Chandramohan V.P.

the operating temperature, flow rate, tube spacing, feeder heights, and other geometrical and flow parameters, which directly influence their performance [5],[6]. The numerical simulations are first validated with data available in the literature. Investigations are also carried out for some other parameters to understand the influence of geometrical and flow parameters on falling film evaporative heat exchangers. In this analysis all three phases; solid, liquid, and gas are simulated by multiphase computational fluid dynamics simulation software. The Volume of Fluid (VOF) model was used, where air represents the primary phase and water represents the second phase. Latent heat, surface tension at the liquid-vapour interface and density difference between the two phases are the most influencing parameters for the heat transfer process. Thus difference induced a buoyancy force that is proportional to the product of gravitational acceleration and the difference between liquid and vapour densities [7].

Reference [8] formulated a bubble nucleation theory in an evaporating falling film heat exchangers. It was suggested that a minimum temperature is required to nucleate boiling. Film thickness influences the rate of falling film heat transfer coefficient. A laser measurement technique is used by [9] to find out the film thickness and its effects on heat transfer. The simulated results in this paper are in good agreement with the optical method and also agree well with the land-mark correlation given by Nusselt. A non-intrusive and optical method has also been developed to avoid contact with liquid film and to find out more accurate results of film thickness over the tubes. In the early phase of the investigation, the film thickness was measured by using a micrometre and found satisfactory agreement with Nusselt theory [10].

Several modern techniques have also been used to measure the range of film thickness and they are all in close agreement [11-15]. Falling film thickness is one of the most important parameters which influence the heat transfer characteristics and hence a simulation is being carried out to investigate the effect of heat transfer coefficient on horizontal circular tubes in the falling film heat exchanger process with varying geometrical and flow parameters. In this paper, a computational fluid dynamics (CFD) simulation has been done to find out the film thickness and heat transfer characteristics around the horizontal tubes. In an earlier study, two geometrical configurations in-line and staggered tube arrangements were investigated and it was observed that the rectangular pitch arrangements show better results [16].

An experimental study for enhancement of falling film evaporation on structured and smooth tube bundles was carried out [17]. Another study has concluded that rolled work tube has better heat transfer compared to other enhanced tubes [18,19]. Characteristics of heat transfer and augmentation of rate of heat transfer coefficient with different geometrical shape with gravity effect was carried out by [20-22].

Besides different geometrical arrangements, some other parameters like tube spacing feeder height, film flow rate, etc. have also been a great area of interest for research to investigate the effect on film heat transfer coefficient [23].

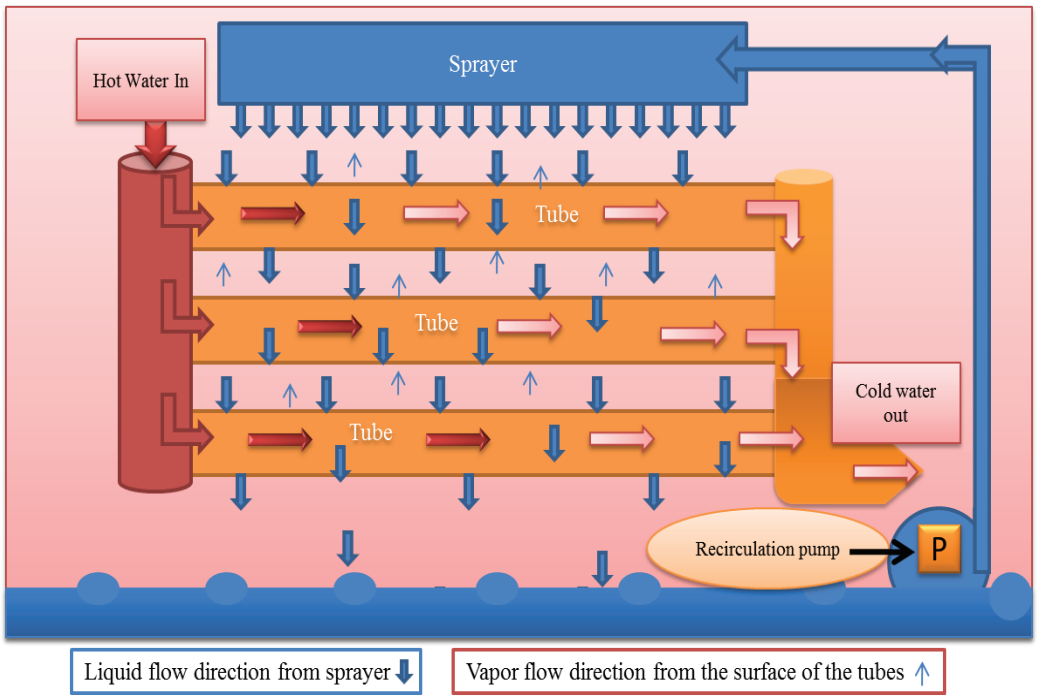

Figure 1. Schematic view of falling film evaporator.

The objective of this paper is to analyze in detail the flow characteristics and heat transfer phenomenon. The interaction of three-phase media is modelled by robust simulation software, and a number of parameters are studied by validating with available data in the literature.

PROBLEM FORMULATION

Problem Set-Up

Computational domains are set up for two-dimensional (2D) as well as three-dimensional (3D) models. Further, the two-dimensional (2D) models are also considered with and without heat transfer. Figure 1 shows three in-line horizontal cylinders are placed horizontally with specified spacing between them. [24] introduced a powerful technique based upon the Fractional Volume of Fluid which describes the free boundary condition. In this numerical simulation, the VOF model is used. Water and air are subdivided into fluid fractions; water is assigned a fluid fraction of 1 whereas air have a fluid fraction of 0.

Boundary Conditions

The boundary conditions for the 2D flow are presented in Figure 2 (a) and visualization of flow domain in 3D model is shown in Figure 2 (b). For reducing the cost of simulation, half of the domain is considered so that it minimizes the grid elements and hence faster simulation can be achieved. In all the cases the cylinder is taken as hollow, because the analysis is focused on the outer surface of the cylinders only.

Mesh Generation

Mesh generation plays a very crucial part in simulation analysis. A sound quality mesh is very essential to capture all the required parameters and satisfy the adopted convergence criteria. Different views of mesh are presented in Figures 3(a), 3(b) and 3(c). The inflation technique is used to precisely capture the liquid film thickness around the cylinder. In this technique, the grid size increases progressively with distance, so that the flow parameters can be captured easily where they are required the most.

Grid Independence Test

The grid independence test has been carried out separately for 2D and 3D models by considering a constant rate of flow. For the 2D model, 57505, 46576 & 31462 numbers of grid points and for the 3D model 355605, 215780 & 110590 numbers of grid points have been used. The results are compared by considering the above grids and it is found that there is variation of less than 5% in the simulation results when moving from finer grid to the finest grid for both 2D and 3D cases. For 2D model 46576 and for 3D model 215780 number of grid points have been taken for further simulation. Time independence test has also been conducted for both models. Three time steps: 0.0022s,

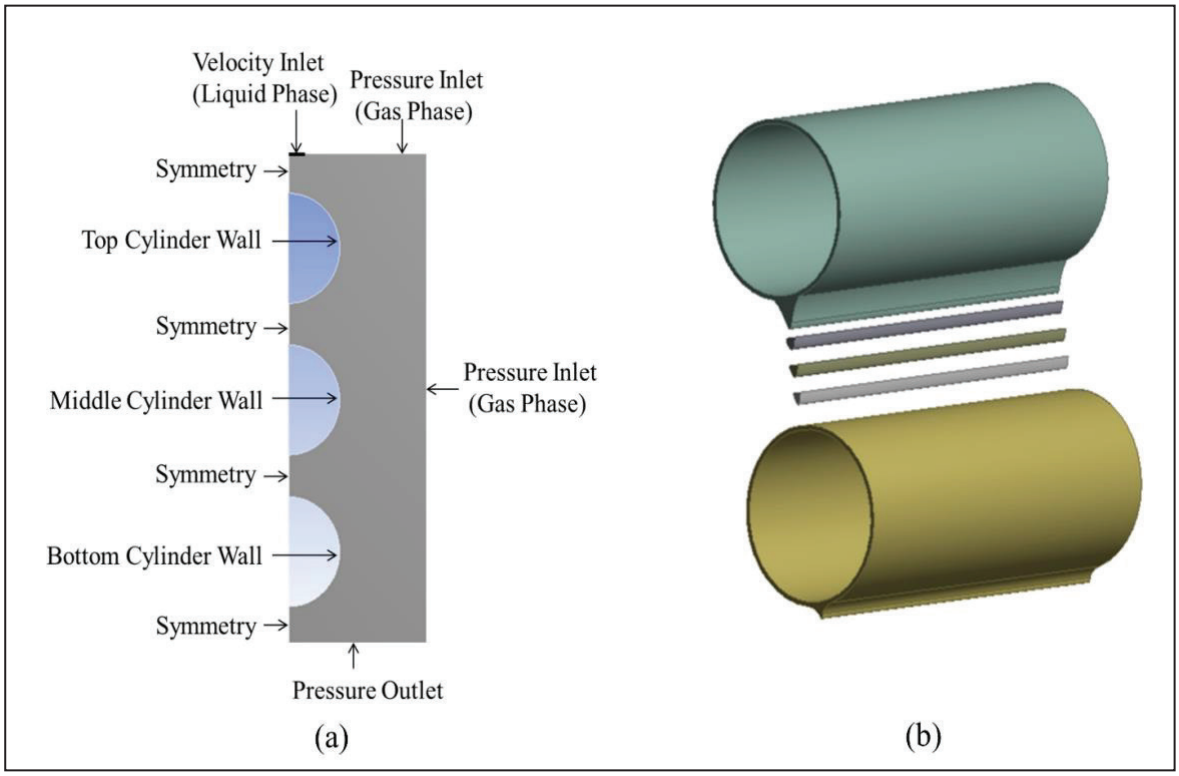

Figure 2. (a) Flow domain and boundary conditions (b) Visualization of the 3D flow.

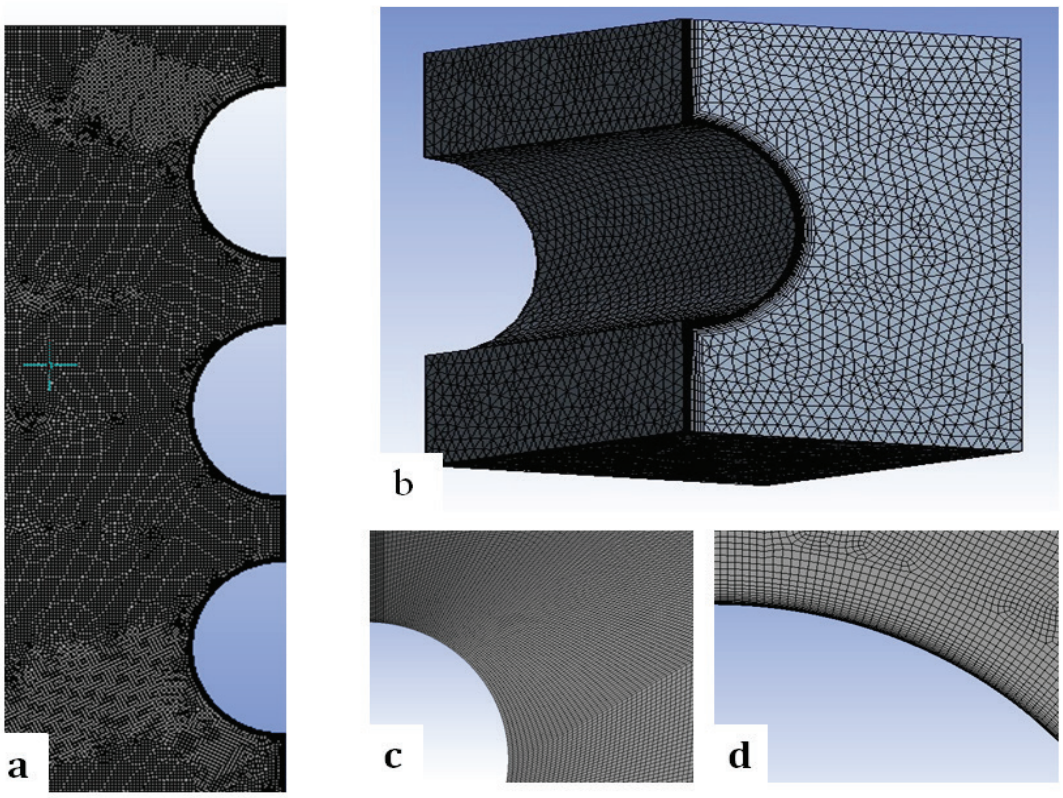

Figure 3. (a) Mesh domain (b) 3D Mesh (c) Mesh with inflation (d) Mapped face meshing.

0.0015s and 0.0005s have been taken and the results are compared. It has been observed further that there is variation of less than 6% in the simulation results when moving from 0.0015s to 0.0005s hence a time step of 0.0015s has been selected for further simulation.

Governing equations to be used in the simulation are:

Conservation of mass equation:

$$\frac{\partial \rho}{\partial t} + \nabla.(\rho \vec{V}) = 0 \tag{1}$$

Momentum equation:

X - component

$$\frac{\partial(\rho u)}{\partial t} + \nabla\cdot(\rho u\vec{V}) = -\frac{\partial p}{\partial x} + \frac{\partial \tau_{xx}}{\partial x} + \frac{\partial \tau_{yx}}{\partial y} + \rho f_x \tag{2}$$

Y- component:

$$\frac{\partial(\rho v)}{\partial t} + \nabla\cdot(\rho v\vec{V}) = -\frac{\partial p}{\partial y} + \frac{\partial \tau_{xy}}{\partial x} + \frac{\partial \tau_{yy}}{\partial y} + \rho f_y \tag{3}$$

Z- component:

$$\frac{\partial(\rho w)}{\partial t} + \nabla\cdot(\rho w\vec{V}) = -\frac{\partial P}{\partial z} + \frac{\partial \tau_{xz}}{\partial x} + \frac{\partial \tau_{yz}}{\partial y} + \frac{\partial \tau_{zz}}{\partial z} + \rho f_z \tag{4}$$

Material Equation:

$$\frac{\partial(\alpha)}{\partial t} + \vec{v}.\nabla\alpha = 0 \tag{5}$$

Energy Equation:

$$\frac{\partial}{\partial t}\left[\rho\left(e+\frac{V^2}{2}\right)\right] + \nabla\cdot\left[\rho\left(e+\frac{V^2}{2}\vec{V}\right)\right] = \rho\dot{q} + \frac{\partial}{\partial x}\left(k\frac{\partial T}{\partial x}\right) + \frac{\partial}{\partial y}\left(k\frac{\partial T}{\partial y}\right) + \frac{\partial}{\partial z}\left(k\frac{\partial T}{\partial z}\right) - \frac{\partial(up)}{\partial x} - \frac{\partial(vp)}{\partial y} - \frac{\partial(wp)}{\partial z} + \frac{\partial(u\tau_{xx})}{\partial x} + \frac{\partial(u\tau_{yx})}{\partial y} + \frac{\partial(u\tau_{zx})}{\partial x} + \frac{\partial(v\tau_{xy})}{\partial x} + \frac{\partial(v\tau_{yy})}{\partial y} + \frac{\partial(v\tau_{zy})}{\partial z} + \frac{\partial(w\tau_{xz})}{\partial x} + \frac{\partial(w\tau_{yz})}{\partial y} + \frac{\partial(w\tau_{zz})}{\partial z} + \rho\vec{f}\cdot\vec{V} \tag{6}$$

Volume Fraction Equation:

$$\rho = \alpha_l \rho_l + \alpha_G \rho_G \tag{7}$$

$$\mu = \alpha_l \mu_l + \alpha_G \mu_G \tag{8}$$

RESULTS AND DISCUSSION

Characteristics of Film Thickness

The formation of film thickness governs the film evaporation from liquid to vapour and conduction and convection heat transfers occurs across the film. Hence it is very

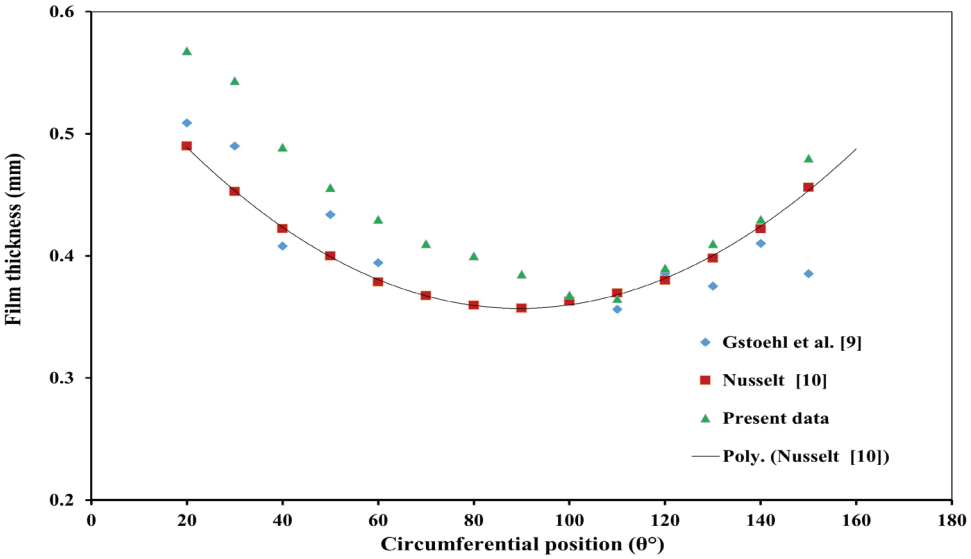

Figure 4. Variation of film thickness at Re_f = 744.

important to study the film formation mechanism and its behaviour and impact on film heat transfer coefficient in falling film heat exchangers. The VOF model is used to investigate the film distribution around the fully wetted horizontal tube. In the numerical simulation, the results were first validated with the Nusselt correlation [10] and data from a non-intrusive optical method adopted by [9] to find the film distribution around the tube. Visualization of film flow and its transient behaviour are captured well and the characteristics of heat flow are simulated for in depth understanding.

The results show good agreement with the experimental results and the comparison has been shown in Figure 4. The film thickness has been simulated around the circumferential angle at film Reynolds number (Re_f =744), with feeder height H=9.5 mm and with tube diameter of 19.05 mm.

Distribution phenomena are captured well by the VOF model and hence it is used for further investigation. The variation of film thickness near the stagnation zone (0° to 35°) of the tube has not been taken into consideration, because in this zone abnormal film thicknesses are observed due to the impingement effect near the stagnation zone. Simulation has also been carried out for film Reynolds number (Re_f =1050) with two tube spacings 9.5 mm and 12.5 mm and with two tube diameters 19.05 mm and 25.05 mm (Figure 5). These tube diameters are generally used for commercial purposes while designing evaporative heat exchangers. The fluid properties were assumed to be constant throughout the process. A marginal variation of film thickness has also been observed when changing the tube diameter from 19.05 mm to 25.05 mm, while all the other parameters were kept constant. This behaviour was also reported by [25] in their experimental observations and it was also observed in a numerical simulation conducted by [26]. In experimental analysis, the film thickness has been measured by using a displacement micrometre. The behavior of film thickness has been studied by varying the feeder height while keeping the Reynolds number and tube diameter constant.

The feeder height plays a major role in determining the hydrodynamic characteristics of the flowing fluid. For different feeder heights it has been observed that the film thickness reduces as the feeder height increases.

Investigations were also performed with a constant feeder height and varying tube diameters. A marginal variation in film thickness has been observed in this case. At greater feeder heights the liquid attains more inertia due to gravity free fall condition and hence attains greater velocity too compared to the lower feeder height satisfying the continuity equation and forming a smaller film thickness around the tube.

The film formation and its visual representation are shown in the Figure 6 (a) and figure 6 (b). Liquid is assumed to flow over the top of the wall, tube diameter is 25.05 mm and the wall of the tube is maintained at constant temperature under normal temperature and pressure conditions. When flow becomes fully developed, an air gap is formed at the end of detachment zone. It occurs due to the inertial motion dominating the adhesion forces and resulting in detachment from the tube wall in early stages.

Transient Behaviour of Flow for Three In-Line Tubes

The flow regimes over three in-line tubes with respect to time have been investigated and shown in Figure 7. The liquid flows down from the top of the tube under the influence of gravity. In the initial stage, at time = 0.17s, the initial impact zone on the top of the tube is shown. Then flow starts moving downwards around the circumference of the tube. In this zone, the moving fluid must overcome pressure

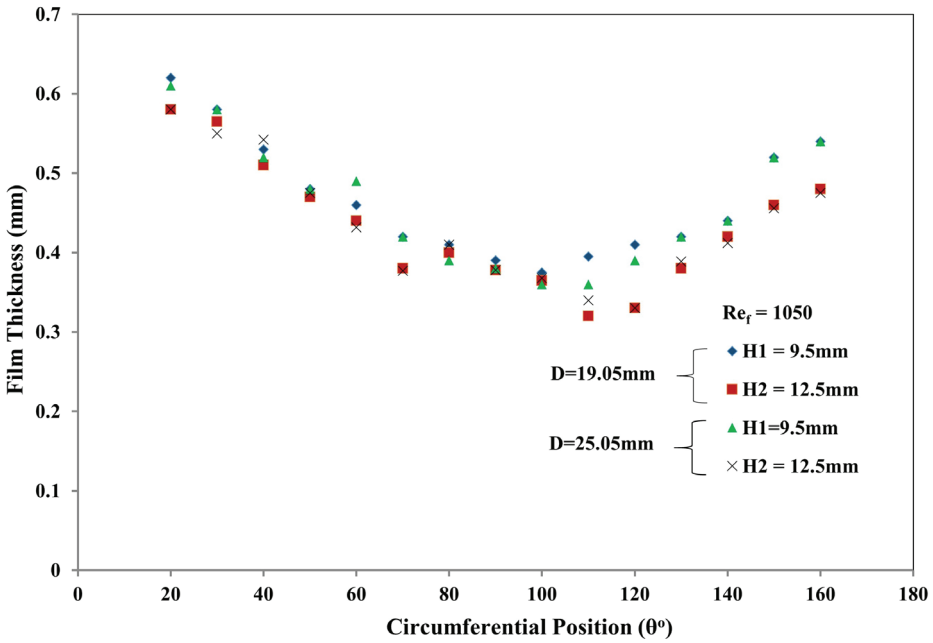

Figure 5. Film thickness at Re_f = 1050.

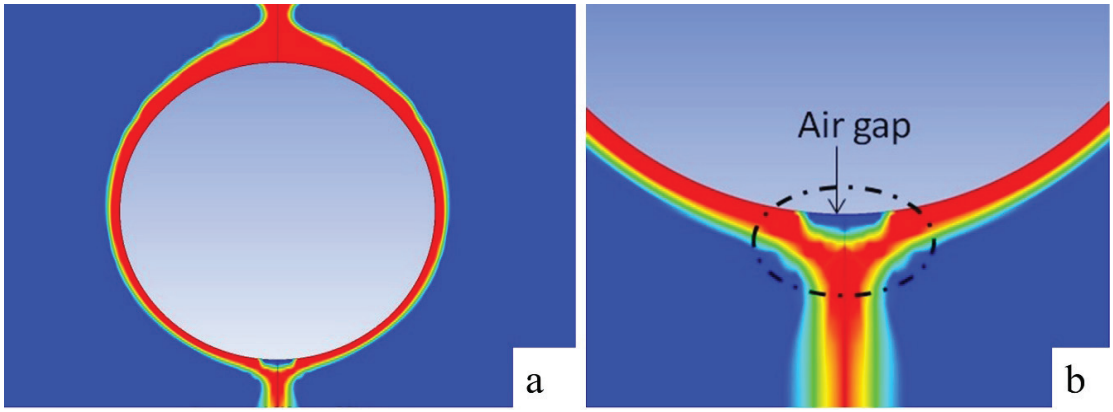

Figure 6. (a) Contours of flow, (b) flow near bottom.

losses due to impact of liquid and the viscous drag between liquid and tube surface for the formation of the liquid film. The different stages of flow have been shown at flow time 0.47s, 0.77s, and 0.88s. The flow covers the tube surface completely at t=1.1s. In this final stage the tube is completely covered by liquid film and then the liquid begins to depart from the bottom of the tube and flows downwards to the top of the lower tube in the form of drops or columns.

Dry Patch Formation

A dry patch formation has also been observed near the bottom of the tube in the 3D simulation carried out at R_f =1050 and outer tube diameter 19.05mm. These patches are quite transient in nature and occur near the bottom of the tube, as shown in Figure 8. The fluctuating patches vary in nature with time and flow rate. At lower flow rates, the formation of dry patches may be quite frequent. The tendency of fouling starts around near the area of occurrence of dry patches.

Wall Shear Stress at Different Circumferential Positions

The variation of shear stress is plotted in Figure 9, the maximum fluctuations are observed near the impingement zone of the tube showing an abnormal behaviour at the bottom of the tube. In the impingement zone, the fluid first comes into contact with the tube surfaces attaining a zero velocity for an instant and then it starts flowing around the tube due to inertial force driven by gravity. This variation accounts for a great deviation in the impingement zone and it occurs around, θ = 0° to 30° of the circumferential position of the tube. The shear stresses show very minimal deviation after the impingement zone and again some abrupt

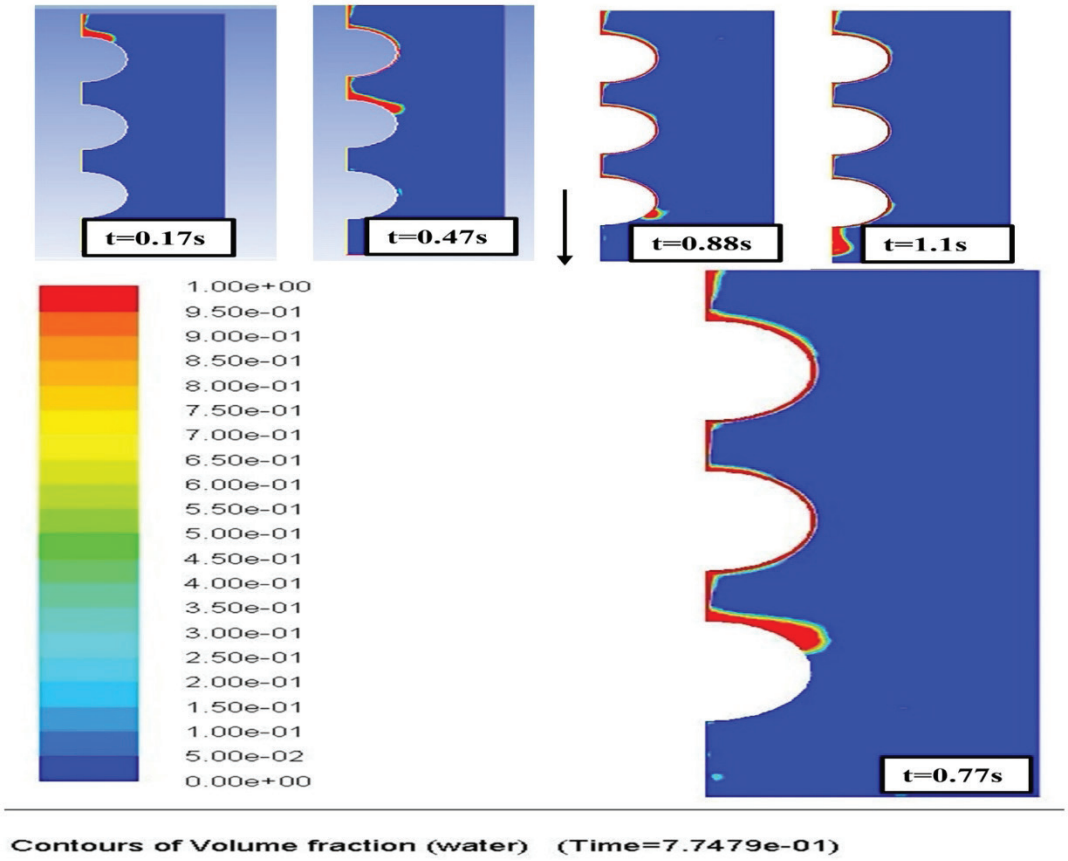

Figure 7. Transient behaviour of flow for three in-line tubes.

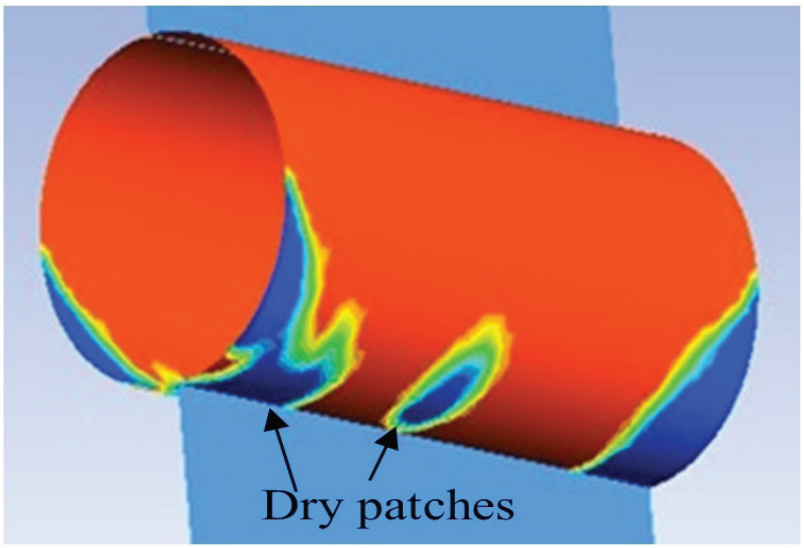

Figure 8. Formation of dry patches.

behaviour is observed in the detachment zone of the tube. Near the detachment zone the fluid is preparing to leave the contact of the tube and hence it shows some abnormal fluctuations of shear stress in the detachment area.

Characteristics of Film Heat Transfer

Heat transfer analysis around the outer surface of tubes of falling film evaporators is carried out by using ANSYS CFD software package. In the present study a single tube of

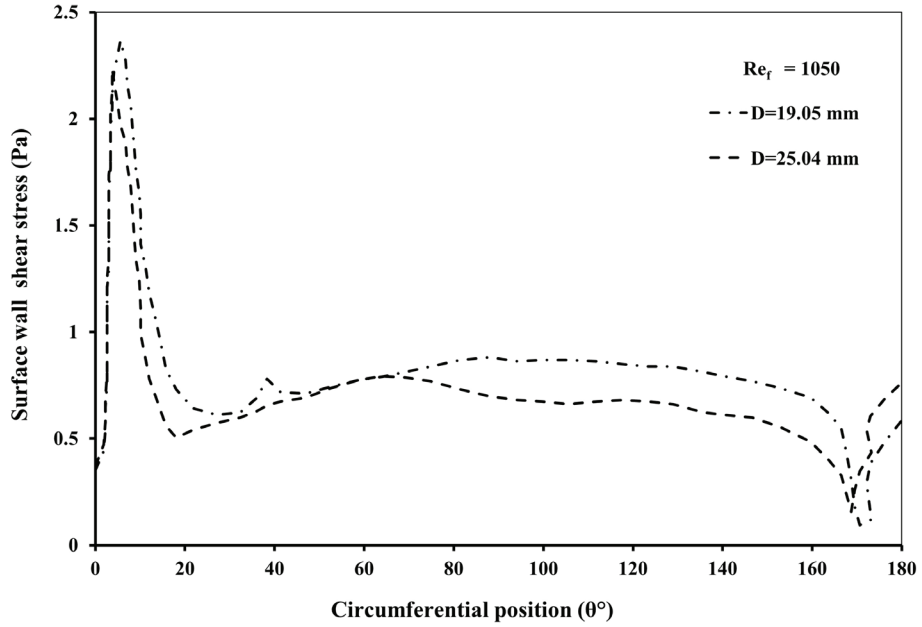

Figure 9. Wall shear stress around circumference of tube.

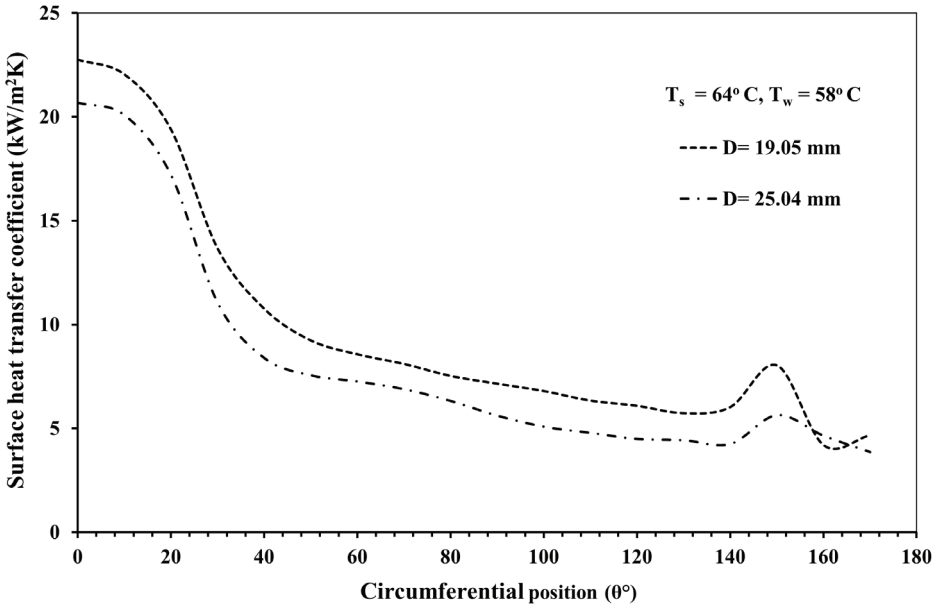

Figure 10. Variation of surface heat transfer coefficient with circumferential position.

diameter 25.05 mm is considered for analysis of convective heat transfer with a two phase VOF model. The temperature at the outer surface is maintained at a constant value and a thin film of water is flowing over the outer surface of the tube under the effect of gravity. The input water film temperature is be maintained constant and the heat transfer parameters are studied. Heat transfer analyses are also carried out by varying the feeder height and surface temperature of the tube.

In this simulation it is assumed that the heat losses due to cumulative effect of surface tension and conduction through the end pipes are negligible and a constant wall temperature is to be maintained for each set of parameters for CFD analysis.

Effect of Tube Diameter on Surface Heat Transfer Coefficient

The surface heat transfer coefficient was investigated for tubes of diameters 19.05 mm and 25.05 mm. The wall

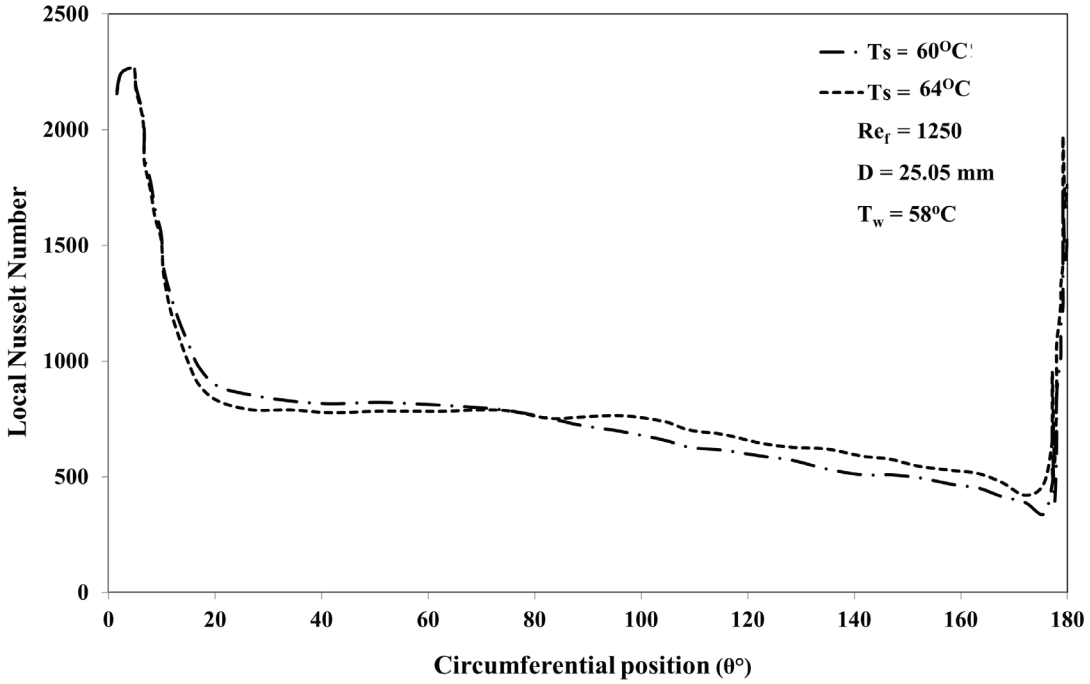

Figure 11. Variation of local Nusselt number with circumferential position.

temperature of tube is kept constant at 64 ˚C and the inlet water temperature was 58 °C. Surface heat transfer coefficients around the tube are plotted in Figure 10**.**

Heat transfer coefficients around the surface of tube are higher near the impingement zone of the tube. It occurs due to the higher temperature received by the fluid near the impingement zone leading to the higher value of heat transfer in this area. Additionally, high gradients in the nascent boundary layer contribute to this. Observations also show that for the smaller tube diameter the value of wall heat transfer is slightly lower as compared to the higher tube diameter. Near the bottom of the tube, fluid is preparing to leave the tube surfaces and shows unpredictable behaviour in this region.

Effect of Tube Wall Superheat

Figure 11 shows the variation of Nusselt number around the circumference of the tube at different temperatures of the tube surface (T_s = 60 °C & 64 °C), while the inlet temperature of the water was kept constant at 58 °C. Increasing the surface temperature of the tube results in an increase in the operating temperature difference and it directly influences the heat transfer phenomenon. Small variations are observed near the stagnation zone of the tube for different surface temperatures and then the variation becomes significant. The evaporation is higher at the higher surface temperature of the tube when other parameters like film Reynolds number and tube diameter are kept constant.

CONCLUSION

Numerical simulations are carried out for horizontal tube falling film evaporators with tube diameter 19.05 mm and 25.05 mm. Variation of film thickness has been studied for two tube diameters with different tube spacing. It is observed that as the film Reynolds number increases the film thickness also increases and it decreases when the tube spacing is increased. Transient behaviour of flow around three in-line tubes is investigated and the tendency of formation of dry patches and air gaps is clearly identified.

Wall shear stresses show significant fluctuations near the impingement zone of the fluid and very little variation is observed on changing the tube diameters. Numerical simulations were also carried out for analysis of heat transfer around the falling film evaporator tubes. It is observed that the film heat transfer coefficient decreases with increasing tube diameter. It can be concluded that the present approach of can predict the physical phenomena faithfully and is robust enough to handle the variations incorporated.

NOMENCLATURE

D	Outer diameter of tube, mm.
H	Feeder height, mm.
k	Thermal conductivity, W / m °C
p	Pressure, N/m^2
q	Heat generation per unit volume, W/m^3
Re	Reynolds number.
t	Time, sec

T Temperature, °C.
u Velocity along x direction, m/s
v Velocity along y direction, m/s
w Velocity along z direction, m/s

Greek symbols
$\emptyset$ Circumferential angle over tube
ρ_f Density of liquid. kg/m^3
ρ_G Density of gas. kg/m^3
α Volume fraction
τα Shear stress, N/m^2
μ Fluid viscosity, Pa s

Subscripts
f Water film
s Surface
W Water
G Gas
l Liquid

AUTHORSHIP CONTRIBUTIONS

Authors equally contributed to this work.

DATA AVAILABILITY STATEMENT

The authors confirm that the data that supports the findings of this study are available within the article. Raw data that support the finding of this study are available from the corresponding author, upon reasonable request.

Raw data was generated at the National Institute of Technology, Kurukshetra. Derived data supporting the findings of this study are available from the corresponding author [NKS] on request.

CONFLICT OF INTEREST

The author declared no potential conflicts of interest with respect to the research, authorship, and/or publication of this article.

ETHICS

There are no ethical issues with the publication of this manuscript.

REFERENCES

[1] Wen T, Lu L, He W, Min Y. Fundamentals and applications of CFD technology on analyzing falling film heat and mass exchangers: A comprehensive review. Appl Energy 2020;261:114473. [CrossRef]
[2] Bouman S, Waalewijn R, Jong Pd, Linden HVD. Design of falling-film evaporators in the dairy industry. Int J Dairy Technol 1993;46:100−106. [CrossRef]
[3] Cyklis P. Industrial scale engineering estimation of the heat transfer in falling film juice evaporators. Appl Therm Eng 2017;123:1365−1373. [CrossRef]
[4] Armbruster R, Mitrovic J. Evaporative cooling of a falling water film on horizontal tubes. Exp Therm Fluid Sci 1998;18:183−194. [CrossRef]
[5] Mohammed H, Abed AM, Wahid M. The effects of geometrical parameters of a corrugated channel with in out-of-phase arrangement. Int Comm Heat Mass Transf 2013;40:47−57. [CrossRef]
[6] Karademir H, Özçelik G, Açikgöz Ö, Dalkiliç AS, İnce İT, Meyer J, et al. Comprehensive review on the flow characteristics of two-phase flows in inclined tubes. J Therm Engineer 2021;7:483−549. [CrossRef]
[7] Bergman TL, Incropera FP, DeWitt DP, Lavine AS. Fundamentals of heat and mass transfer. New York: John Wiley & Sons; 2011.
[8] Mitrovic J. Preventing formation of dry patches in seawater falling film evaporators. Desalin Water Treat 2011;29:149−157. [CrossRef]
[9] Gstoehl D, Roques J, Crisinel P, Thome J. Measurement of falling film thickness around a horizontal tube using a laser measurement technique. Heat Transf Engineer 2004;25:28−34. [CrossRef]
[10] Nusselt W. Die Oberflächenkondensation des Wasserdampfes. Z VDI 1916;60:541−546.
[11] Chen J, Zhang R, Niu R. Numerical simulation of horizontal tube bundle falling film flow pattern transformation. Renew Energy 2015;73:62−68. [CrossRef]
[12] Dukler A. Characteristics of flow in falling liquid film. Proc Chem Eng Prog Symp Series 1952;48:557−563.
[13] Abraham R, Mani A. Heat transfer characteristics in horizontal tube bundles for falling film evaporation in multi-effect desalination system. Desalination 2015;375:129−137. [CrossRef]
[14] Wang X, He M, Fan H, Zhang Y. Measurement of falling film thickness around a horizontal tube using laser-induced fluorescence technique. J Phys: Conf Ser 2009;147:012039. [CrossRef]
[15] Liu S, Mu X, Shen S, Li C, Wang B. Experimental study on the distribution of local heat transfer coefficient of falling film heat transfer outside horizontal tube. Int J Heat Mass Transf 2021;170:121031. [CrossRef]
[16] Zhang J, Wang B, Peng X. Falling liquid film thickness measurement by an optical-electronic method. Rev Sci Instrum 2000;71:1883−1886. [CrossRef]
[17] Zhao CY, Ji WT, Jin PH, Zhong YJ, Tao WQ. Experimental study of the local and average falling film evaporation coefficients in a horizontal enhanced tube bundle using R134a. Appl Therm Engineer 2018;129:502−511. [CrossRef]
[18] Liu Z, Yi J. Falling film evaporation heat transfer of water/salt mixtures from roll-worked enhanced tubes and tube bundle. Appl Therm Engineer 2002;22:83−95. [CrossRef]

[19] Pu L, Li Q, Shao X, Ding L, Li Y. Effects of tube shape on flow and heat transfer characteristics in falling film evaporation. Appl Therm Engineer 2019;148:412−419. [CrossRef]
[20] Bayareh M. Numerical simulation and analysis of heat transfer for different geometries of corrugated tubes in a double pipe heat exchanger. J Therm Engineer 2019;5:293−301. [CrossRef]
[21] Panda S, Kumar R. A review on effect of various artificial roughness on heat transfer enhancement in a channel flow. J Therm Engineer 2021;7:1267−12301. [CrossRef]
[22] Sundravel A, Suresh S, Deenadayalan S. Numerical investigation of supercritical heat transfer of water flowing in vertical and horizontal tube with emphasis of gravity effect. J Therm Engineer 2021;7:1541−1555. [CrossRef]
[23] Yan WM, Pan CW, Yang TF, Ghalambaz M. Experimental study on fluid flow and heat transfer characteristics of falling film over tube bundle. Int J Heat Mass Transf 2019;130:9−24. [CrossRef]
[24] Hirt CW, Nichols BD. Volume of fluid (VOF) method for the dynamics of free boundaries. J Comput Phys 1981;39:201−225. [CrossRef]
[25] Hou H, Bi Q, Ma H, Wu G. Distribution characteristics of falling film thickness around a horizontal tube. Desalination 2012;285:393−398. [CrossRef]
[26] Singh N, Kumar Poddar A. Numerical study of liquid film formation around tubes of horizontal falling film evaporator. J Appl Fluid Mech 2021;14:1045−1052. [CrossRef]